

Investigations of pressure-wave action through the exhaust system of a diesel engine

E.M. Abdel Aleem ^a, M.M. Osman ^b, E.A. Marzouk ^b and A.I. Abdel-Fattah ^b

^a Arab Academy for Science and Technology & Maritime Transport, Alexandria 1029, Egypt

^b Mechanical Eng. Dept., Alexandria University, Alexandria 215 44, Egypt

The present research work deals with the pressure waves caused by the unsteady flow of the exhaust system in internal combustion engines, and the effects of various parameters on the behavior of these waves and its effects on engine performance. A theoretical investigation of some numerical solutions for the unsteady flow and their application to the exhaust system of internal combustion engines was carried out. A numerical model was developed to solve the unsteady flow of the exhaust system for a single cylinder 4-stroke diesel engine, depending on Benson methodology of "Homotropic Flow Field", in which the entropy of the flow field is assumed to be uniform and constant. The research includes an experimental work on the test diesel engine recording the pressure wave patterns and amplitudes through the exhaust pipe at three positions. The pressure was recorded by a strain gauge absolute pressure transducer with built in amplifier attached to digital oscilloscope. The paper demonstrates the influence of pressure wave created through the exhaust system of a diesel engines on engine performance, the effect of changes in engine speed, load, exhaust pipe end configuration, the valve area ratio on pressure wave action were investigated.

يهدف هذا البحث الى دراسة الموجات التضاغية الناتجة من السريان الغير مستقر المتولد في نظام الطرد لمحركات الاحتراق الداخلي ودراسة تأثير ظروف التشغيل المختلفة للمحرك وكذلك التغير في تصميم نظام الطرد على طبيعة تلك الموجات ومدى تأثير ذلك على كفاءة أداء المحرك. وقد تضمن البحث دراسة نظرية شاملة لنظام الطرد لمحرك احتراق داخلي رباعية الأشواط ذو اسطوانة واحدة يعمل بوقود الديزل وذو ماسورة طرد واحدة. شملت الدراسة الدورة الحرارية للمحرك والتغير في الضغط ودرجات الحرارة داخل الاسطوانة وحساب سرعة سريان غازات العادم خلال ماسورة الطرد لوضع التقييم الأولى للموجات التضاغية المتولدة خلال فترة الإندفاع المتتالي لغازات العادم من خلال صمام العادم الى ماسورة الطرد. كما تطرق البحث الى إجراء دراسة نظرية لبعض طرق الحل العددي المستخدمة في حل معادلات السريان الغير مستقر وما يختص منها بحل سريان غازات العادم لمحركات الاحتراق الداخلي. ومن خلال تلك الدراسة تم تطوير نموذج عددي احادي البعد يعتمد على طريقة الخصائص المعدلة لبيسون لحل السريان الغير مستقر لمحرك احتراق داخلي رباعي الأشواط ذات ماسورة طرد واحدة. بعد إهمال التغير في الإنتروبي والإنتقال الحراري والإحتكاك مع الوضع في الاعتبار التغير في مساحة مقطع مخرج ماسورة الطرد. حيث امكن بواسطة هذا النموذج الحصول على القيم التقديرية لجميع خصائص السريان خلال ماسورة الطرد عند ظروف تشغيل مختلفة للمحرك وعند مقاطع مختلفة لنهاية ماسورة الطرد. كما امكن أيضا من خلال هذا النموذج الحصول على التغير في شكل الضغط داخل الاسطوانة أثناء شوط الطرد. كما شمل البحث أيضا تجارب معملية على المحرك المذكور تم خلالها قياس الموجات التضاغية المتتالية الناتجة عن السريان الغير مستقر لنظام الطرد للمحرك وذلك خلال ماسورة الطرد في ثلاث مواقع تبدأ مباشرة ومنتصف الماسورة ونهايتها باستخدام جهاز رصد الموجات التضاغية مع جهاز مبين الموجات الرقمي والمحتوى على جهاز رسم الموجات وقد تم تسجيل شكل وقيمة الموجات التضاغية عمليا خلال عدة تجارب شملت التشغيل الخارجة للمحرك دون إشعال لرصد طبيعة الموجات في حالة السريان الغير مستقر دون التغير في الإنتروبي. التشغيل الفعلي للمحرك مع الوضع في الاعتبار ظروف تشغيل مختلفة مثل السرعة والحمل وكذلك التغير في تصميم ماسورة الطرد. هذ وقد تمت المقارنة بين النتائج المعملية والنتائج النظرية للنموذج العددي لكلا الحالتين وكانت النتيجة هذه المقارنة مرضية.

Keywords: Diesel engines, Exhaust system, Pressure-wave

1. Introduction

It is known that the power developed by the internal combustion engine directly depends on the quantity of air available. One of the effective methods for increasing the intake charge is the intake and exhaust

system tuning. The pressure waves initiated during the induction and exhaust processes affect the engine operation and thus engine performance. The events of pressure waves initiated through tuned exhaust pipe intend to reduce the exhaust back pressure and thus

improve the scavenging process improving combustion and reduce engine emissions.

The effect of pressure wave action through inlet and exhaust manifolds can be calculated by the use of numerical methods, with development solutions of conservation equations and efficient shock-capturing schemes for the non-steady flow through ducts, and also can be measured by actual experimental work on test engines.

Bannister and Macklow [1] developed the finite wave theory of Earnshaw [2] and applied it to the sudden release of gas from a cylinder, and later to engine conditions. The method allowed the calculation of finite amplitude interaction.

Riemann [3] suggested solving the method of characteristics by proposing a technique, which caters for waves traveling in both directions.

De Haller [4] applied the method of characteristics to the exhaust systems of an engines and Jenny [5] extended it to include area change friction and heat transfer.

Woods and Kenn [6] confirmed the constant pressure model for valves experimentally under cold conditions, whereby; Benson and Galloway [7] confirmed under engine test conditions. Kastiner [8] used an isentropic flow model for the flow through valve.

Shapiro [9] derived the governing equations of one dimensional unsteady compressible flow with friction and heat transfer.

Rowland Benson [10] used a high-speed digital computer to analyze the wave action in a single-cylinder supercharged two-stroke engine considering friction, heat transfer, variable entropy and gradual area changes. Marzouk et al. [11] showed that the modified method of characteristics of Spalding is highly recommended for the description and analysis of all the inherently discontinuous unsteady flow.

In the present study the equations of unsteady compressible flow field have been solved by designed model and an experimental work was carried on a test engine in the I.C.E. laboratory of the Mechanical Engineering Department at Alexandria University. The objective of the work reported here was to investigate the effects of pressure wave action

created through the exhaust system of I.C.E. at different engine working conditions and with use of different exhaust pipe end configurations, and to compare the numerical model results with those obtained experimentally.

2. Theoretical analysis of the pressure wave action through the exhaust system of internal combustion engine

A theoretical analysis of pressure wave was created through a single exhaust pipe of diesel 4-stroke single cylinder were done based on the following operating conditions:-

1. Engine running speed 1200 r.p.m.
 2. Exhaust pipe length 1.0 meter.
 3. Exhaust pipe diameter 55 mm.
 4. The exhaust valve opens at 125° A.T.D.C.
 5. The cylinder pressure at the moment of blow-down is 3.5 bars.
 6. Engine bore × stroke = 90 × 125 mm.
 7. No shock wave occurs in the exhaust pipe.
- The crank revolution / s = 1200/60 = 20 rev/s. Thus the degree of crank / s = 360 × 20 = 7200°/s.

The calculation of the pressure wave values depends on:

- i. Calculation of exhaust gas speed at exhaust pipe entrance based on piston speed and area ratio " $\Psi = A_v / A_p$ ".
- ii. Prediction of exhaust gas energy during the blow down period from engine thermal cycle (T-S) chart for diesel engine fig. 1 and applying the energy equation:

$$u_{exv} = \sqrt{\frac{2gj(H_i - H_7)}{28}} \quad (1)$$

Where: H_i Exhaust gas energy inside the cylinder during the blow down period at corresponding points "6, a, b, c, d" in kcal/kmol. fig. 2. H_7 . Exhaust gas energy at (B.D.C.) in kcal /kmol.

The pressure wave at the exhaust pipe entrance calculated from the following equation:

$$P_p = \rho_g a \mu_{exp} \quad (2)$$

Where:

ρ_g exhaust gas density
" a " local speed of sound at exhaust pipe

entrance.

$$= 20 \sqrt{T} \quad \text{assuming } T = 500 \text{ }^\circ\text{K.} \quad a = 446 \text{ m/sec}$$

$$\mu_{exp} = 0.35 \mu_{ev} \text{ depending on valve area ratio } \Psi$$

The pressure wave value has been calculated for three conditions of pipe end configuration, fully open end, partially open end 30% reflection, and fully closed end exhaust pipe. Table 1 and fig. 2 present the results of the above calculations.

3. Numerical solution of non-steady compressible flow through exhaust system of internal combustion engine

The one dimensional unsteady compressible flow is described by differential equations derived from basic conservation equations of mass, momentum and energy, [9], which represent the flow field through a con-

trol volume fig. 3, is given by the following equation:

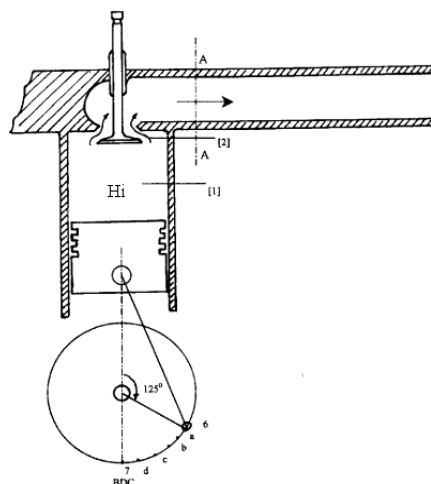


Fig. 1. Schematic diagram for out flow through exhaust valve during blow-down period.

Table 1

The pressure wave values at section (A-A) of exhaust pipe during the blow down period

Crank angle	Exhaust gas conditions			Press. wave value at section "A-A" $P = \rho a u_{exp}$ kg/cm ²	Reflection time $\Delta t = 2L/a$ sec $L = 1.0$ m	Corresponds crank angle degree $\alpha = \Delta t \times 7200$	The super position crank angle	Press. value of 30% refl. partially open end kg/cm ²	Press. value of 100% refl. Fully closed end pipe kg/cm ²
	Exh. gas density ρg kg/m ³	Acoustic speed through exhaust pipe "a" m/sec	Exhaust gas velocity u_{exp} m/sec						
125°	1.5	446	243	1.62	0.00448	34.5	159	0.48	1.62
130°	1.5	446	220	1.47	0.0038	34.5	164	0.44	1.47
135°	1.47	446	195	1.27	0.0034	34.5	169	0.38	1.27
140°	1.45	446	185	1.19	0.00346	34.5	174	0.35	1.19
145°	1.41	446	180	1.13	0.0035	34.5	179	0.33	1.13
150°	1.40	446	177	1.10	0.00353	34.5	184	0.33	1.10
155°	1.10	446	160	0.78	0.00357	34.5	189	0.23	0.78
160°	0.95	446	150	0.63	0.0036	34.5	194	0.18	0.63
165°	0.80	446	132	0.47	0.0036	34.5	199	0.14	0.47
170°	0.75	446	120	0.40	0.00373	34.5	204	0.12	0.40
175°	0.70	446	83	0.26	0.0038	34.5	209	0.07	0.26
180°	0.70	446	80	0.24	0.0038	34.5	214	0.07	0.24

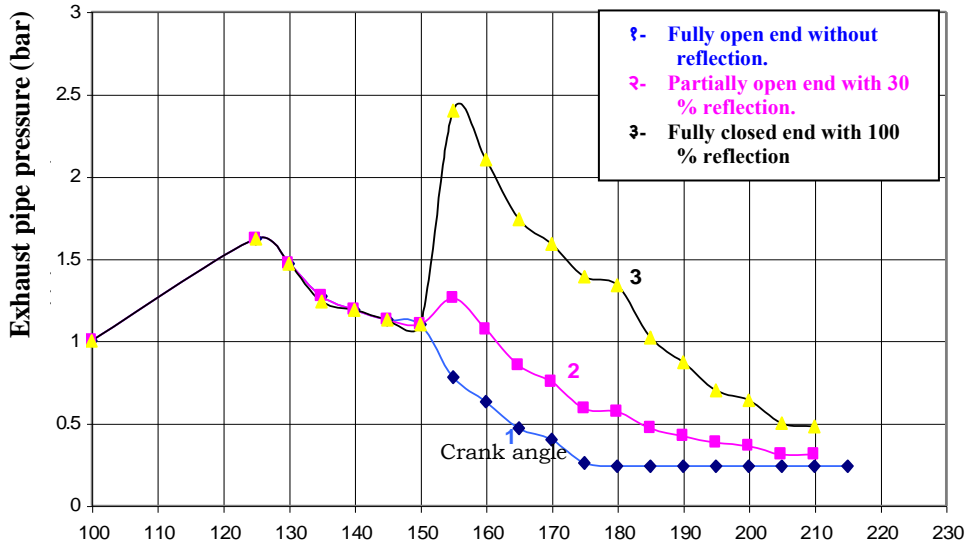


Fig. 2. The pressure wave valves against crank shaft angle with different exhaust pipe end configurations.

$$\frac{\partial}{\partial t} \left\{ \begin{matrix} \rho \\ \rho u \\ \rho \left(e + \frac{u^2}{2} \right) \end{matrix} \right\} + \frac{\partial}{\partial x} \left\{ \begin{matrix} \rho u \\ \rho u^2 + p \\ \rho u \left(e + \frac{u^2}{2} + \frac{p}{\rho} \right) \end{matrix} \right\} = \left\{ \begin{matrix} -\frac{\rho u}{Ar} \frac{dAr}{dx} \\ -\rho G - \frac{\rho u^2}{Ar} \frac{dAr}{dx} \\ \rho q - \frac{1}{Ar} \left\{ \rho u \left(e + \frac{p}{\rho} + \frac{u^2}{2} \right) \frac{dAr}{dx} \right\} \end{matrix} \right\} \quad (3)$$

where:

G is the friction force per unit mass of fluid,
 F is the fanning friction coefficient, and
 Q is the heat transfer per unit mass of fluid.
 All are given by refs. [12, 13].

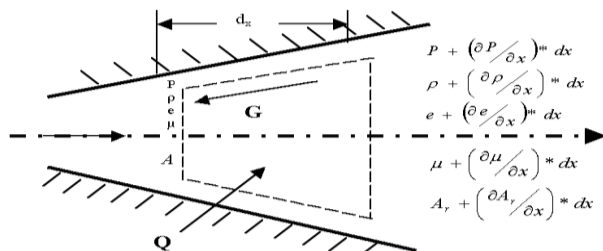


Fig. 3. One-dimensional flow through an infinitesimal control volume in a variable area duct.

The above system of eq. (3) is transformed by its characteristic form as clarified by ref. [13] with use of the method of characteristics [5]. The equations solved algebraically to find the values of the dependent variables at the new time level for internal nodes as shown in fig. 4.

The final form of the characteristics equations which represents the flow field without approximation is given by [13, 14].

$$d \left[a + \frac{\gamma-1}{2} \mu \right] = \frac{a^2}{2C_p} \left[\frac{\partial s}{\partial x} - \rho \frac{RG}{P} \right] dt + \frac{\gamma-1}{2} a \rho \left[\frac{q+uG}{P} \right] dt - \frac{\gamma-1}{2} \frac{a \mu}{Ar} \frac{dAr}{dx} dt \quad (4)$$

Where:

$$d = \left[\frac{\partial}{\partial t} + (\mu + a) \frac{\partial}{\partial x} \right] dt \quad \text{along slop } \frac{1}{\mu + a}$$

and

$$d \left[a - \frac{\gamma-1}{2} \mu \right] = \frac{\gamma-1}{2} a \rho \left[\frac{q + \mu G}{P} \right] dt - \frac{a^2}{2C_p} \left[\frac{\partial s}{\partial x} - \rho \frac{RG}{P} \right] dt - \frac{\gamma-1}{2} \frac{a \mu}{Ar} \frac{dAr}{dx} dt \quad (5)$$

Where:

$$d = \left[\frac{\partial}{\partial t} + (\mu - a) \frac{\partial}{\partial x} \right] dt \text{ along slop } \frac{1}{\mu - a}$$

and

$$ds = R\rho \left[\frac{q + \mu G}{P} \right] dt . \quad (6)$$

Where:

$$d = \left[\frac{\partial}{\partial t} + \mu \frac{\partial}{\partial x} \right] dt \text{ along slope } \frac{1}{\mu}$$

There are two versions have been carried out as numerical methods for solving these equations, one was introduced by Benson [10], and the other was by Spalding [12]. In this study a designed model based on Benson methodology for homentropic flow field has been introduced.

4. Benson methodology for homentropic flow field

The numerical solution of Benson [13] is performed wholly in the position diagram “z-x field”, which is subdivided into a rectangular grid system, fig. 5. The grid pattern is fixed in

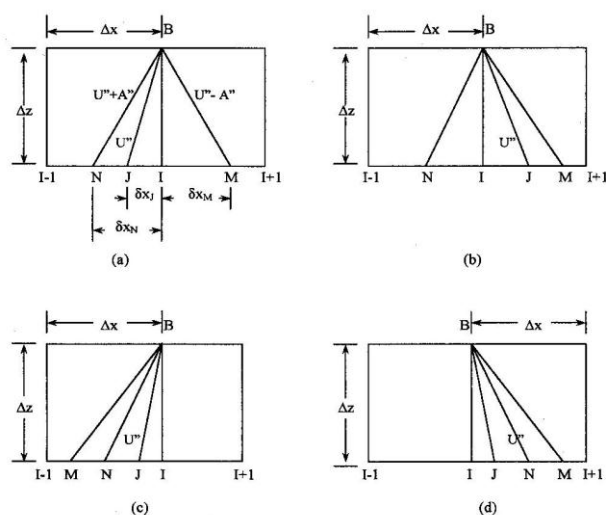


Fig. 4. Characteristics slopes imposed on a fixed grid system for the modified method of Spalding. (a) subsonic flow (U'' Positive) (b) subsonic flow (U'' negative) (c) supersonic flow (U'' positive) (d) supersonic flow (U'' negative).

the x-direction but the time step “z” is adjusted according to the stability criterion;

$$\frac{\Delta Z}{\Delta X} \leq \frac{1}{A + |U|} .$$

Benson [10] introduced the generalized characteristics λ_I and λ_{II} where λ_I is the characteristic whose nominal slope is from left to right in a duct, and λ_{II} is a characteristic whose nominal slope is from right to left. The basic equations for evaluation of general characteristic λ_I and λ_{II} given as follows:

$$(\lambda_I)_{r+1,s} = (\lambda_I)_{r,s} + \frac{\Delta Z}{\Delta X} \left\{ b(\lambda_I)_{r,s-1} - a(\lambda_{II})_{r,s-1} \right\}^* \left\{ (\lambda_I)_{r,s-1} - (\lambda_I)_{r,s} \right\} \quad (7)$$

$$(\lambda_{II})_{r+1,s} = (\lambda_{II})_{r,s} + \frac{\Delta Z}{\Delta X} \left\{ b(\lambda_{II})_{r,s+1} - a(\lambda_I)_{r,s+1} \right\}^* \left\{ (\lambda_{II})_{r,s+1} - (\lambda_{II})_{r,s} \right\} . \quad (8)$$

5. The theoretical model

The application of the digital computer to solve the non-steady flow problems was made by Benson, Garg and Woolatt [16], this technique has proved successful in solving the non-steady flow problems in internal combustion engines, the method is applicable to both homentropic and non-homentropic flows. In this study the flow considered to be isentropic flow, thus the characteristics equations have been reduced to the following equations:

$$\frac{\partial}{\partial t} \left[a + \frac{k-1}{2} \mu \right] + (\mu + a) \frac{\partial}{\partial x} \left[a + \frac{k-1}{2} \mu \right] = 0 \quad (9)$$

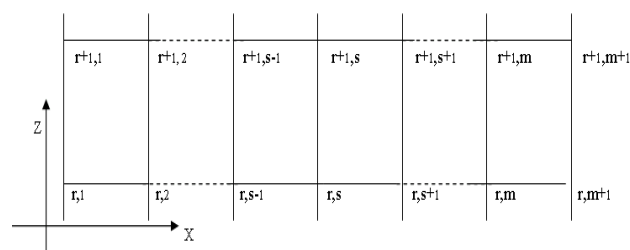


Fig. 5. Subdivision of pipe into meshes in z-x plane.

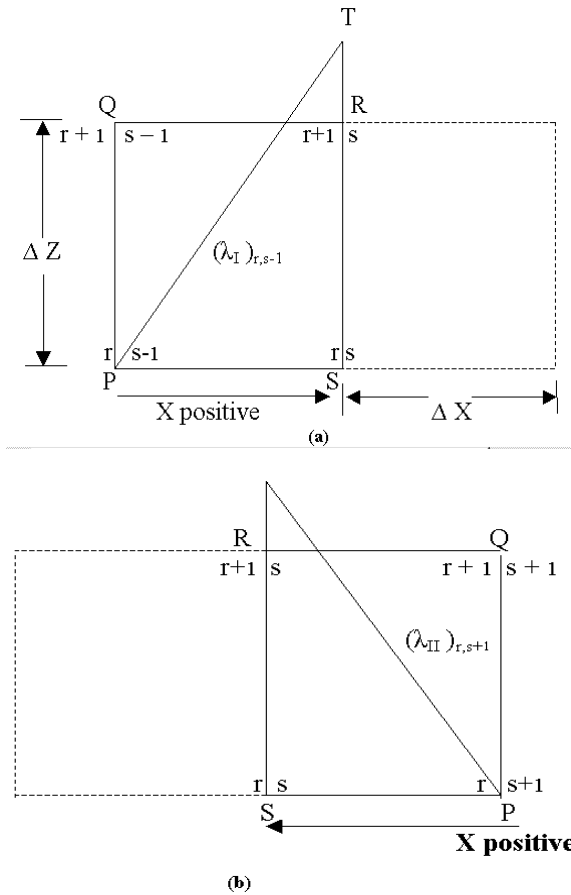


Fig. 6-a, b. Benson method for evaluation of the Riemann variable (a) λ_I b- λ_{II} .

$$\frac{\partial}{\partial t} \left[a - \frac{k-1}{2} \mu \right] + (\mu - a) \frac{\partial}{\partial x} \left[a - \frac{k-1}{2} \mu \right] = 0 \quad (10)$$

A computer program structure for single-cylinder engine with single exhaust pipe has been designed to solve the flow field of exhaust system "Homotropic System" using Benson Methodology [13]. The program solves the system during one cycle, i.e. 720° of crank angle; the time step is set in degrees of crank angle. Logical decisions are made to check the calculation at any point and adjust the angle when it exceeds 720° , and test is done on valve opening and closing time incorporated with valve area-crank angle degrees, after the valve areas have been determined the cylinder pressure is calculated from the previous

cylinder pressure and rate of change of pressure using simple Euler integration:

$$\frac{dP_c}{dt} = \frac{1}{V_c} \left\{ a_{0a}^2 \left(\frac{dm}{dt} \right)_a - a_c^a \left(\frac{dm}{dt} \right)_e - k P_c \left(\frac{dV_c}{dt} \right) \right\} \quad (11)$$

and

$$\frac{dV_c}{dt} = F_c r \left[\sin \theta + \frac{1}{2} \left\{ \frac{\sin 2\theta}{\sqrt{(n^2 - \sin^2 \theta)}} \right\} \right] 2\pi N \quad (12)$$

Where:

- F_c Cylinder cross sectional area,
- R Crank radius = stroke / 2,
- N Connecting Rod length / crank radius,
- θ Crank angle from T.D.C., and
- CR Nominal compression ratio.

The mass flow rate out of a cylinder can be calculated from the following eq. Benson [13].

$$m' = \rho_2 \mu_2 F_2$$

$$\frac{dm_e}{dt} = k \left(\frac{P_{ref}}{a_{ref}} \right) F \frac{U}{A^2} P \times 10^5 \text{ kg/sec.} \quad (13)$$

A Fortran subroutine for the valve has been established during program running, the valve area ratio ψ is tested. If it is zero, the valve is closed and if ψ is greater than 1.0 then it is set equal to unity, at that time the flow is then controlled by the pipe and not the valve.

6. The program structure

The basic structure comprises four stages as follows:

Stage two: It contains the data input, the form of data output and the formulation of the reference conditions. The boundary condition equations are subroutines and their data, if required are included in the first stage.

Second one: is the calculation of the time step ΔZ from the stability criterion, followed by the evaluation of all the Riemann variables at the mesh points using eqs. (7) and (8). This is followed immediately by:

Stage Three: comprises the calculation of the boundary values " λ_{out} " at each end from the boundary equation subroutines.

Stage Four: is the final stage including print out the results and transfer of the Riemann variables at the mesh points for the next time step. If the calculation is not completed the process is repeated by returning to stage two, the determination of the next time step.

7. The experimental work procedures

The pressure waves were recorded at three positions on the exhaust pipe of tested engine A, B, C at distance intervals of 6, 52, 96 cm from exhaust port exit, the experiments were done for two engine working conditions: Engine Motoring Test and Engine Firing Test fig. 7 presents the experimental set up schematic diagram and table 2 lists the test equipments used during the experiments, table 3 presents the test engine technical data and specification.

7.1. Engine motoring test results

In this test the pressure wave pattern was recorded experimentally while engine motored at speed of 900 and 1000 r.p.m. and with use of exhaust pipe length 1.0 m only fully open end pipe. Fig. 8-a, b shows the numerical and experimental results of pressure wave pattern during this test. Fig. 9-a, b and fig. 10-a, b present the calculation results of mathematical model for cylinder pressure mass flow rate and the exhaust gas velocity at locations A, B and C through the exhaust pipe. The analysis of engine motoring test results shows that the wave reflection through exhaust pipe causes the pressure to be dropped below the atmospheric pressure. Also the wave amplitude increases as engine speed increases.

The analysis shows that the gas velocity reaches its maximum value at pipe exit and some wave events presented inside cylinder due to the sudden opening of the exhaust valve and the mass flow rate shows some improvement as engine speed increased.

7.2. Engine firing test results

In this test the pressure wave was recorded while engine firing at speeds of 1000, 1200 r.p.m. and engine full load. The first

group of engine firing test was done with use of exhaust pipe length $L = 1.0$ m and the second group was done with use of exhaust pipe length $L = 1.5$ m.

The conditions of exhaust pipe end were as follows:

1) Fully open end. 2) Convergent nozzle end $d_{th} = 30$ mm. $\theta = 54$ %. 3) Convergent nozzle end exhaust pipe $d_{th} = 20$ mm. $\theta = 36$ %, nozzle length = 60 mm. 4) Convergent divergent nozzle end exhaust pipe $d_{th} = 20$ mm. $\theta = 36$ %.

Table 4 presents the results comparisons of the pressure wave during these tests, and fig. 11-a, b, fig. 12-a, 12-b and fig. 13 present the result comparison of pressure wave pattern at position "A". The analysis of these test results shows the following remarks:

- The calculated results of pressure wave from fluid dynamic model agreed favorably with the experimental measurements values.
- The experimental results show that the pressure wave amplitude increases as engine speed and load increases.
- The results also show that by inserting a convergent nozzle at pipe end the suction wave reflection decreases but exhaust gas velocity at pipe end increases.

The second group of engine firing test was done at the same engine operating conditions but with different exhaust pipe length ($L = 1.5$ m) and with use of divergent nozzle end (diffuser cone angle 10° and length 0.7 m). The numerical and experimental results of these tests are summarized in table 5, fig. 15-a,b,c presents the pressure wave pattern comparison at position "A" while engine firing at 1000, 1200 r.p.m. and full load, with use of fully open end exhaust pipe, while fig. 16-a,b,c. presents the pressure wave pattern comparison at position "A" with use of divergent end exhaust pipe.

The result analysis of these group tests show that the exhaust pipe length has a great effect on the pressure wave action through exhaust system of internal combustion engine and inserting divergent nozzle (diffuser) at pipe end improves the positive events of the pressure wave action since during these tests the suction wave reflection amplitude shows a reasonable increase.

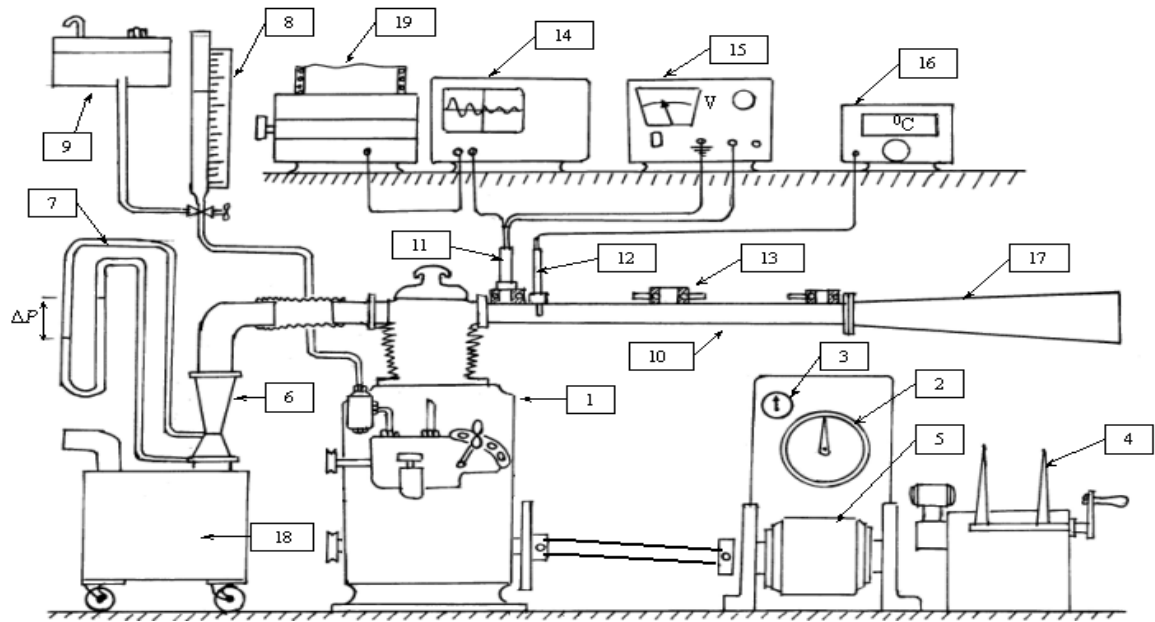


Fig. 7. Schematic diagram of the experimental setup and measuring equipments.

Table 2
The test equipments used during the experiments

Equipment no.	Description
1	Engine
2	Dynamometer "Torque Indicator"
3	Engine speed indicator "r.p.m"
4	Liquid control rheostat
5	Dynamometer "electric motor – generator"
6	Venturi flow meter " for measuring air flow rate"
7	Water tube manometer
8	Fuel meter scale
9	Fuel tank
10	Exhaust pipe
11	Strain gauge pressure transducer
12	Thermocouple thermometer
13	Pressure transducer attached nut with cooling circuit
14	Oscilloscope "Digital"
15	AC/DC Adaptor
16	Thermocouple read out "mill voltmeter"
17	Diffuser
18	Air Tank
19	Printer

(A) Engine Motoring Test Results

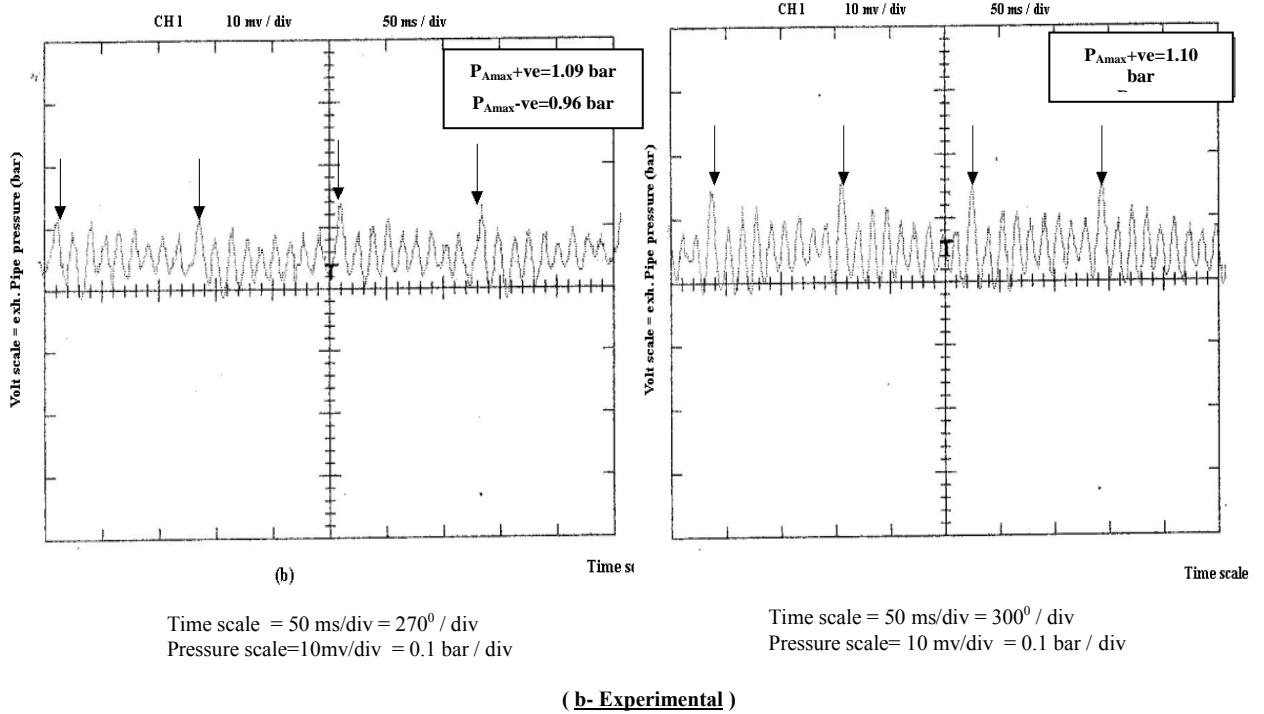
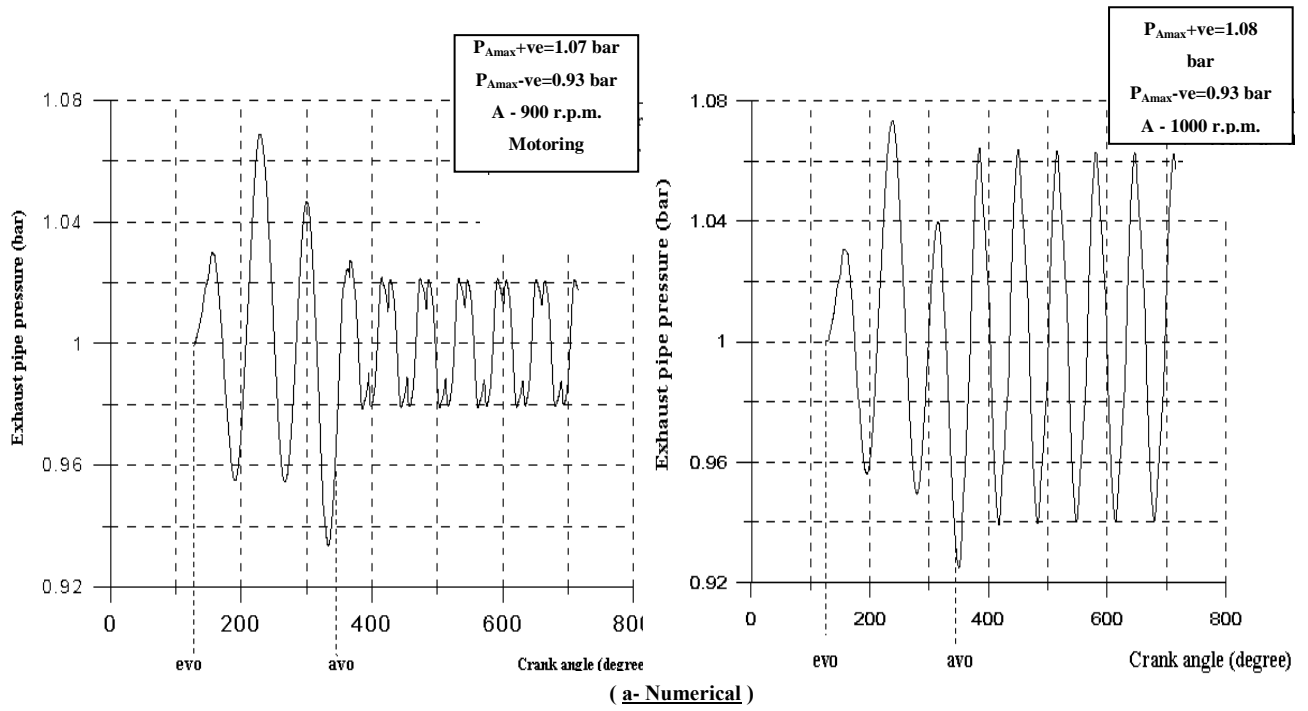
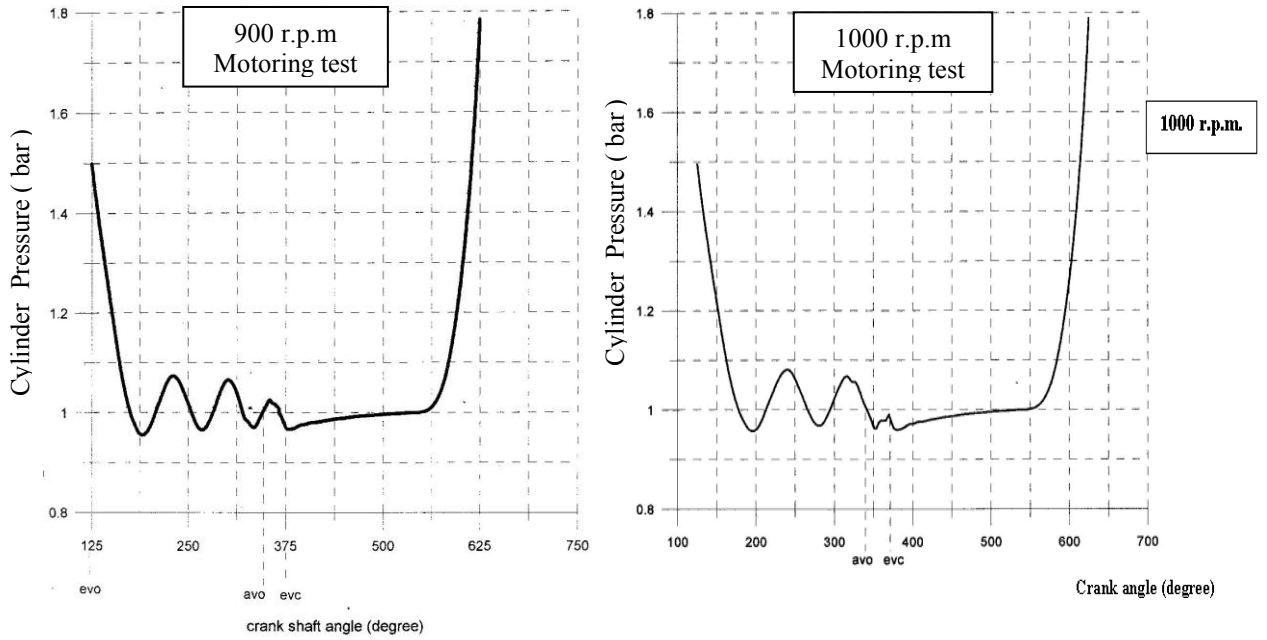
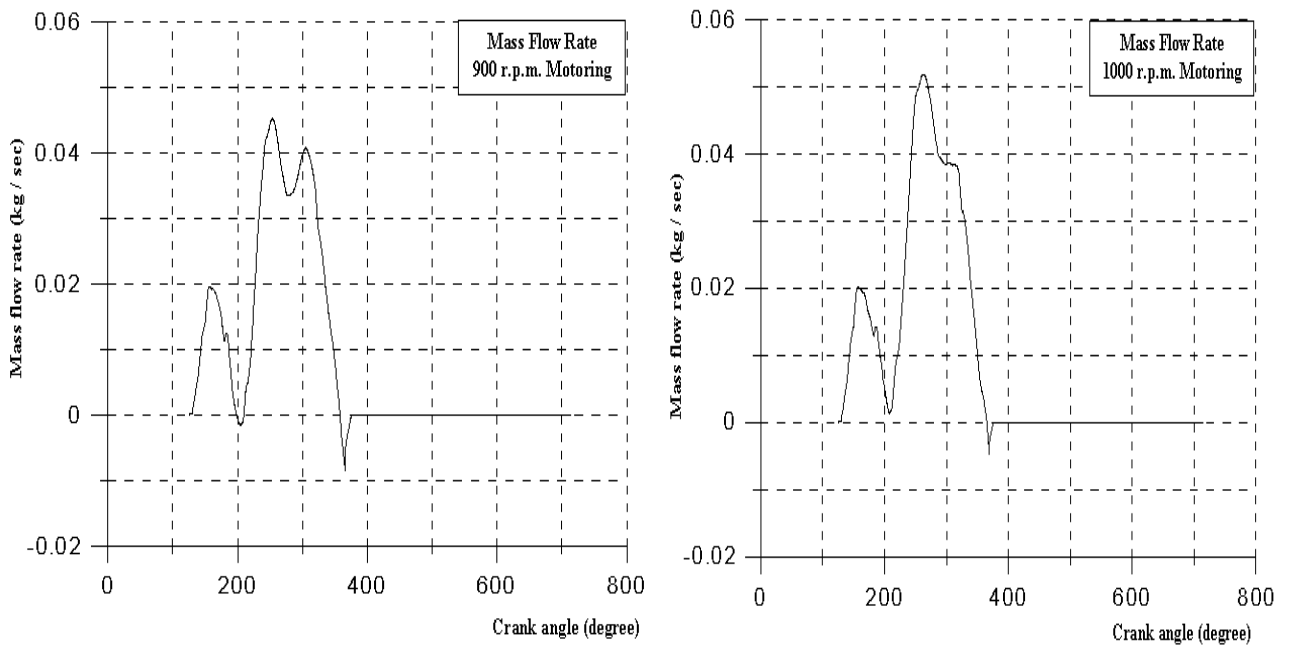


Fig. 8-a,b. Numerical and experimental results of pressure wave pattern at position "A" when engine motoring at speed of 900, 1000 r.p.m.

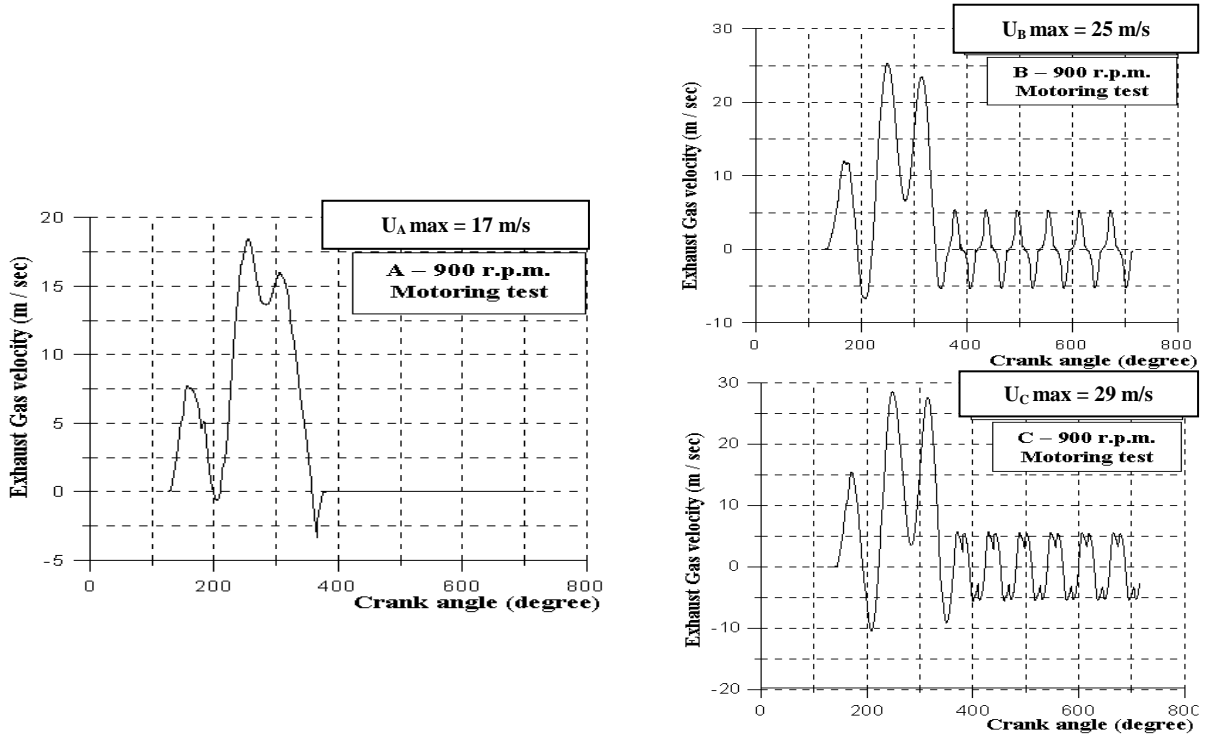


(a- Cylinder Pressure)

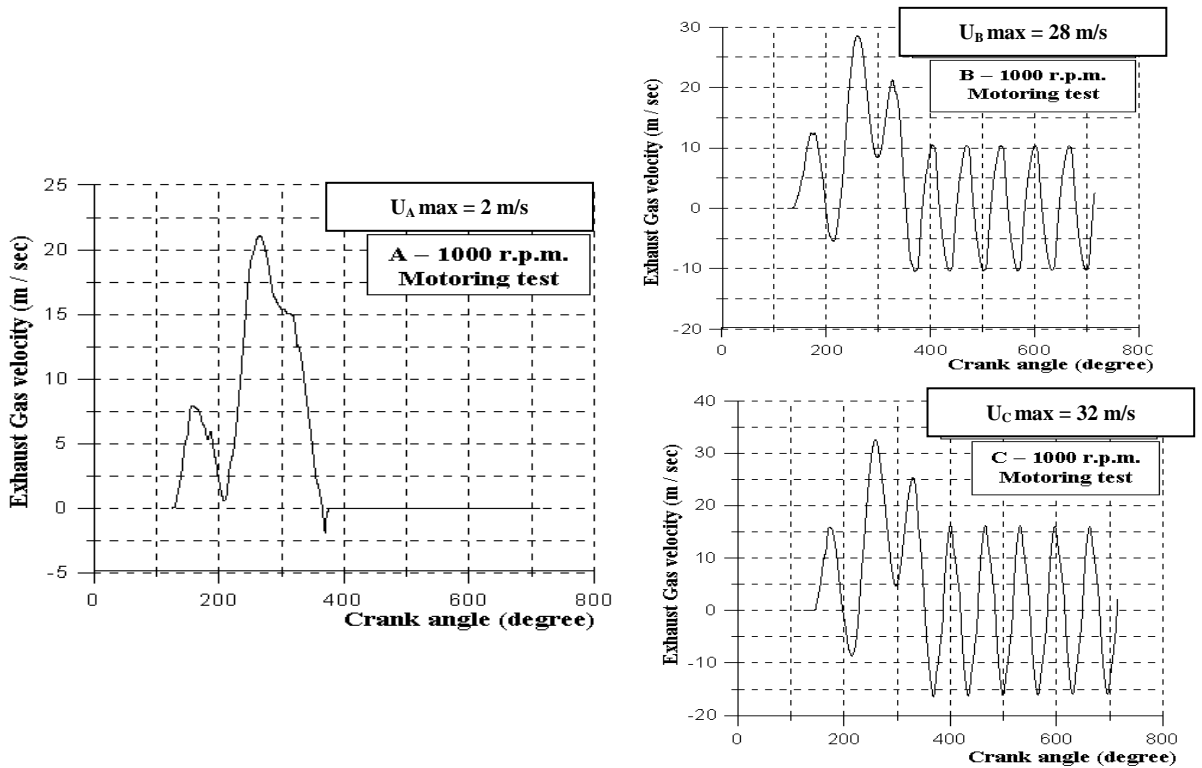


(b- Mass Flow Rate)

Fig. 9-a, b. Numerical results of cylinder pressure and exhaust gas mass flow rate while engine motoring at speed of 900 and 1000 r.p.m.



(a) Positions A, B and C at Speed 900 r.p.m.



(b) Positions A, B and C at Speed 1000 r.p.m.

Fig. 10-a, b. Comparison of exhaust gas velocity at positions A, B, C while engine motored at speed of 900 and 1000 r.p.m.

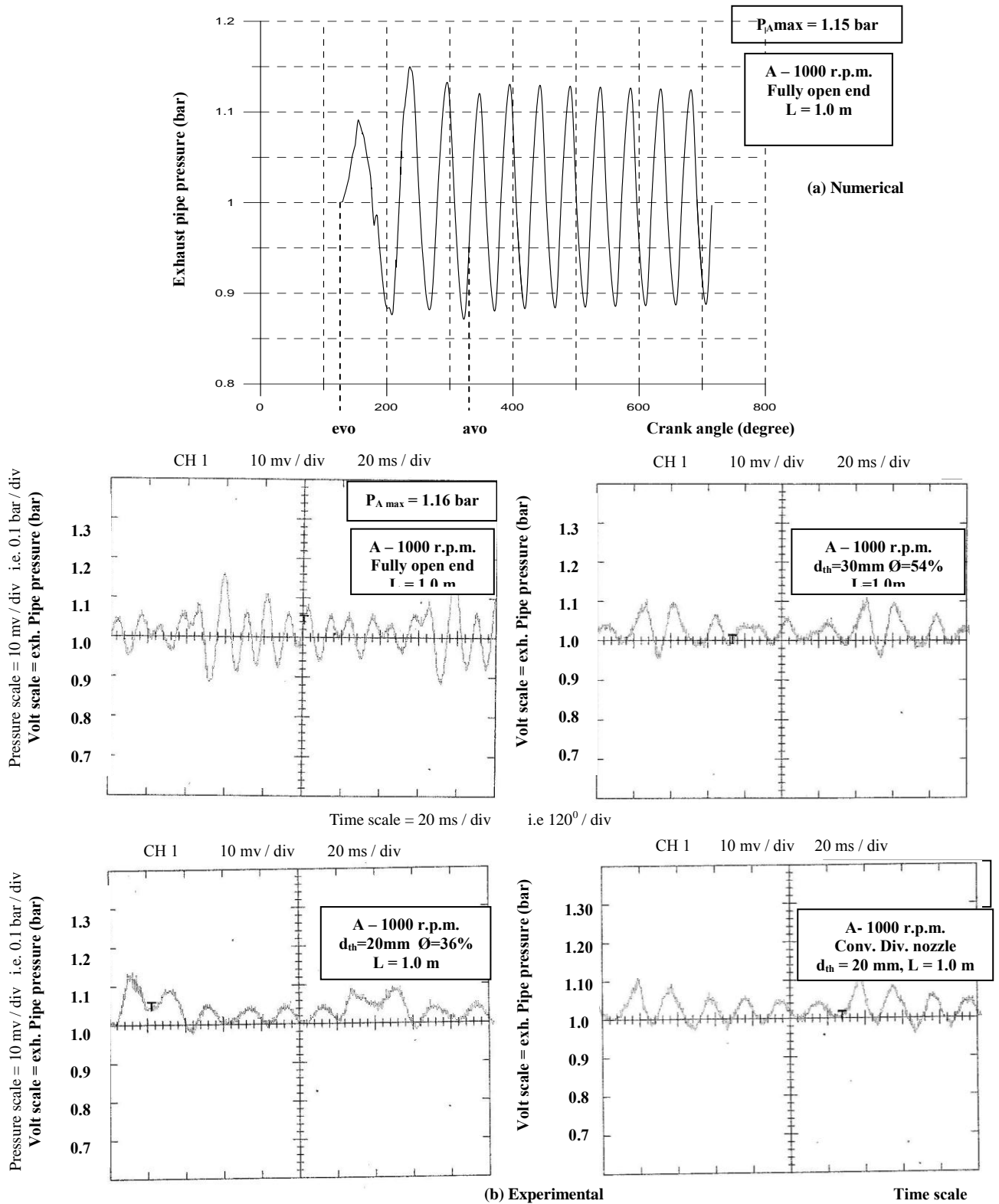


Fig. 11-a, b. Comparison of pressure wave pattern while engine firing with different exhaust pipe end configuration at speed 1000 r.p.m.

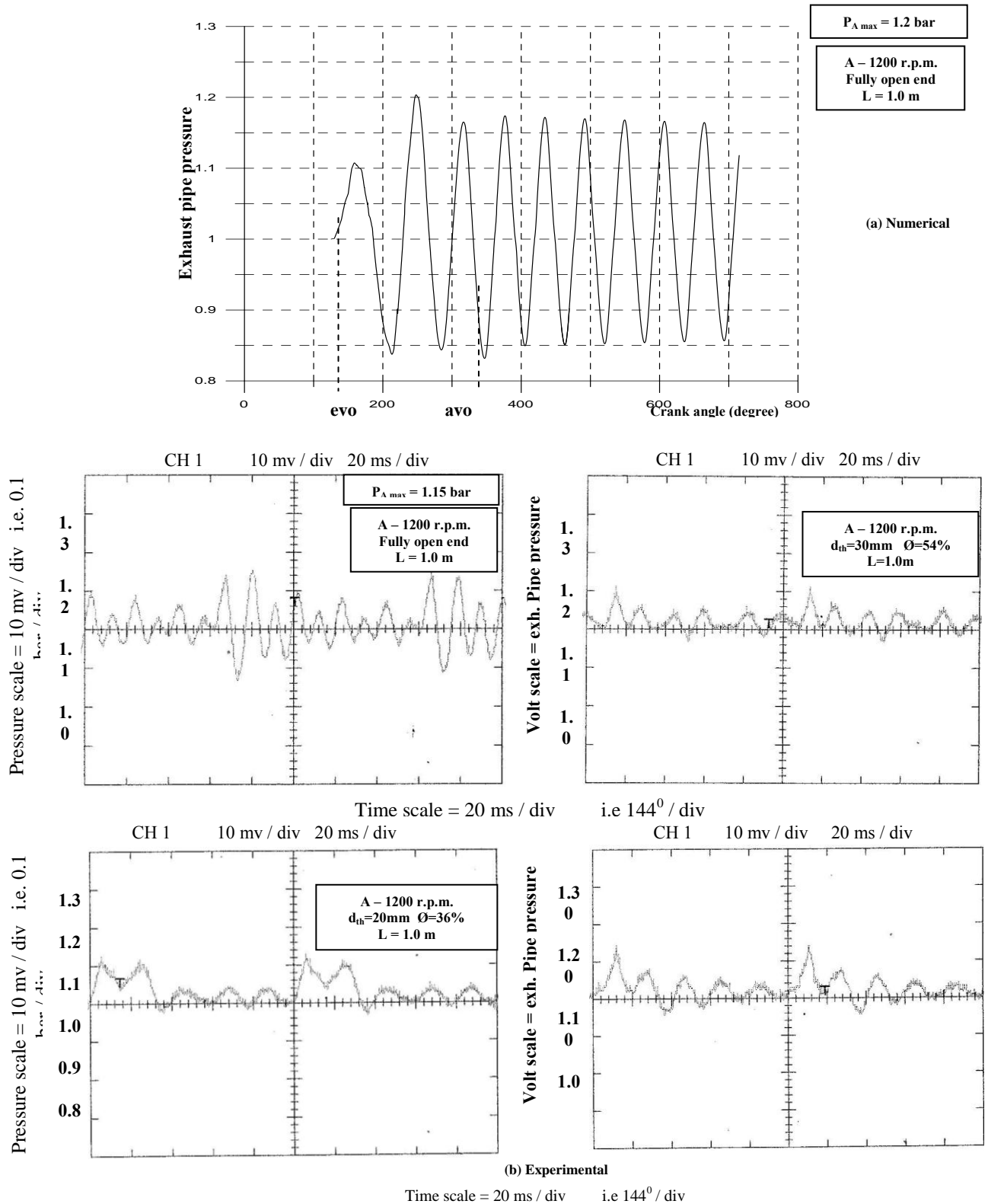


Fig. 12-a, b. Comparison of pressure wave pattern while engine firing with different exhaust pipe end configuration at speed 1200 r.p.m.

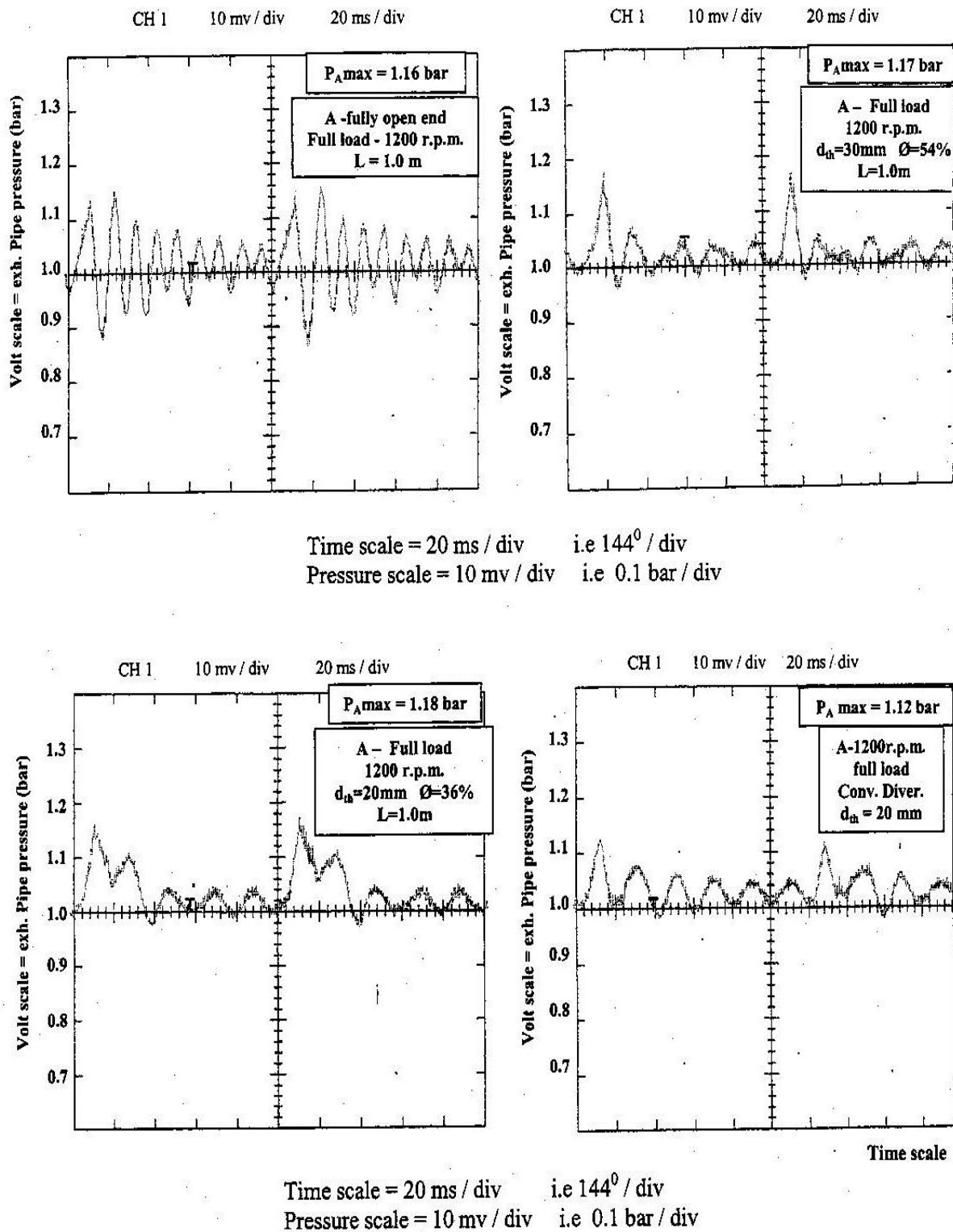


Fig. 13. Comparison of pressure wave pattern while engine firing with different exhaust pipe end configuration at full load- 1200 r.p.m.

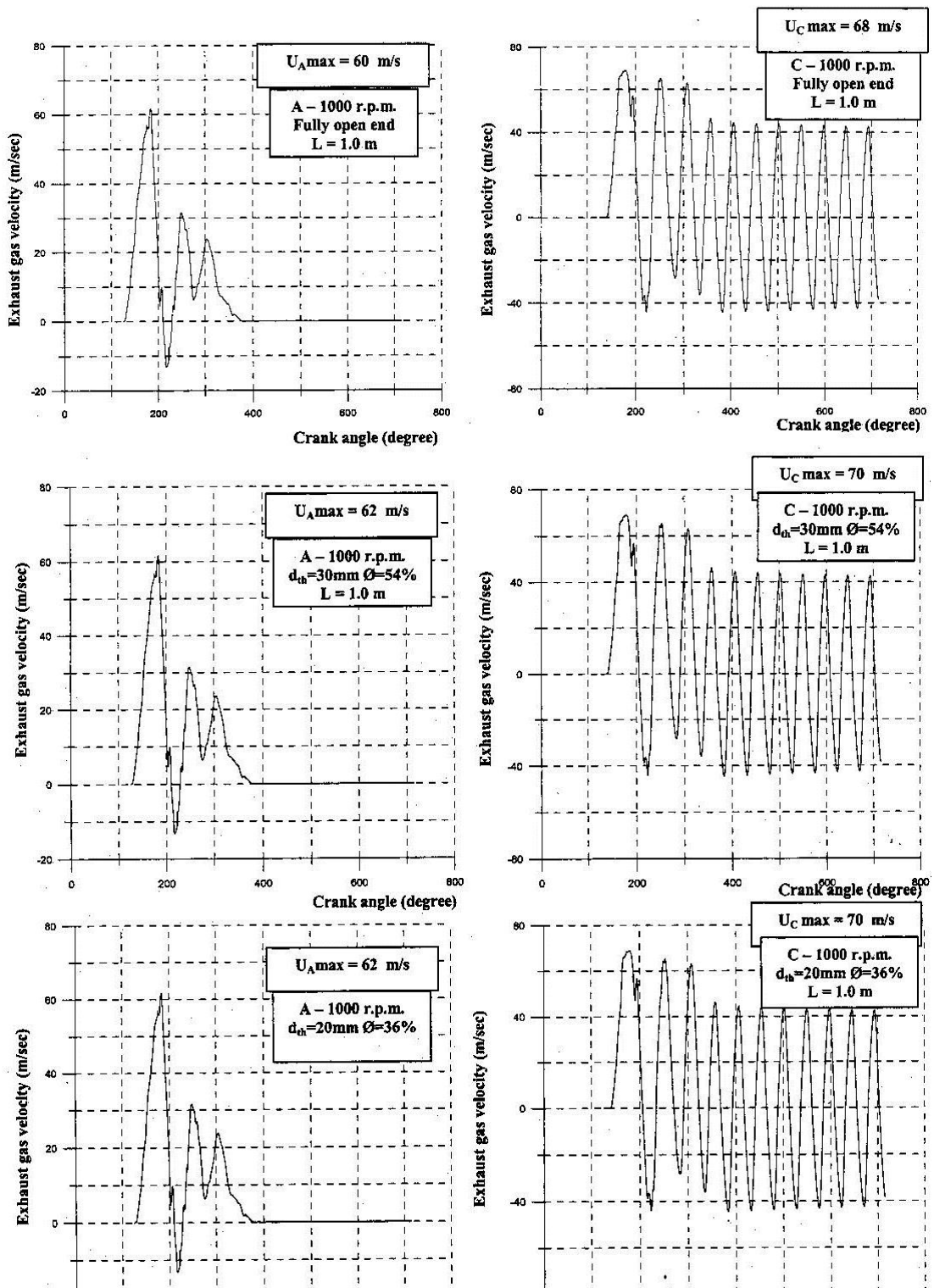


Fig. 14. Comparison of exhaust gas velocity while engine firing with different exhaust pipe end configuration at positions A and C.

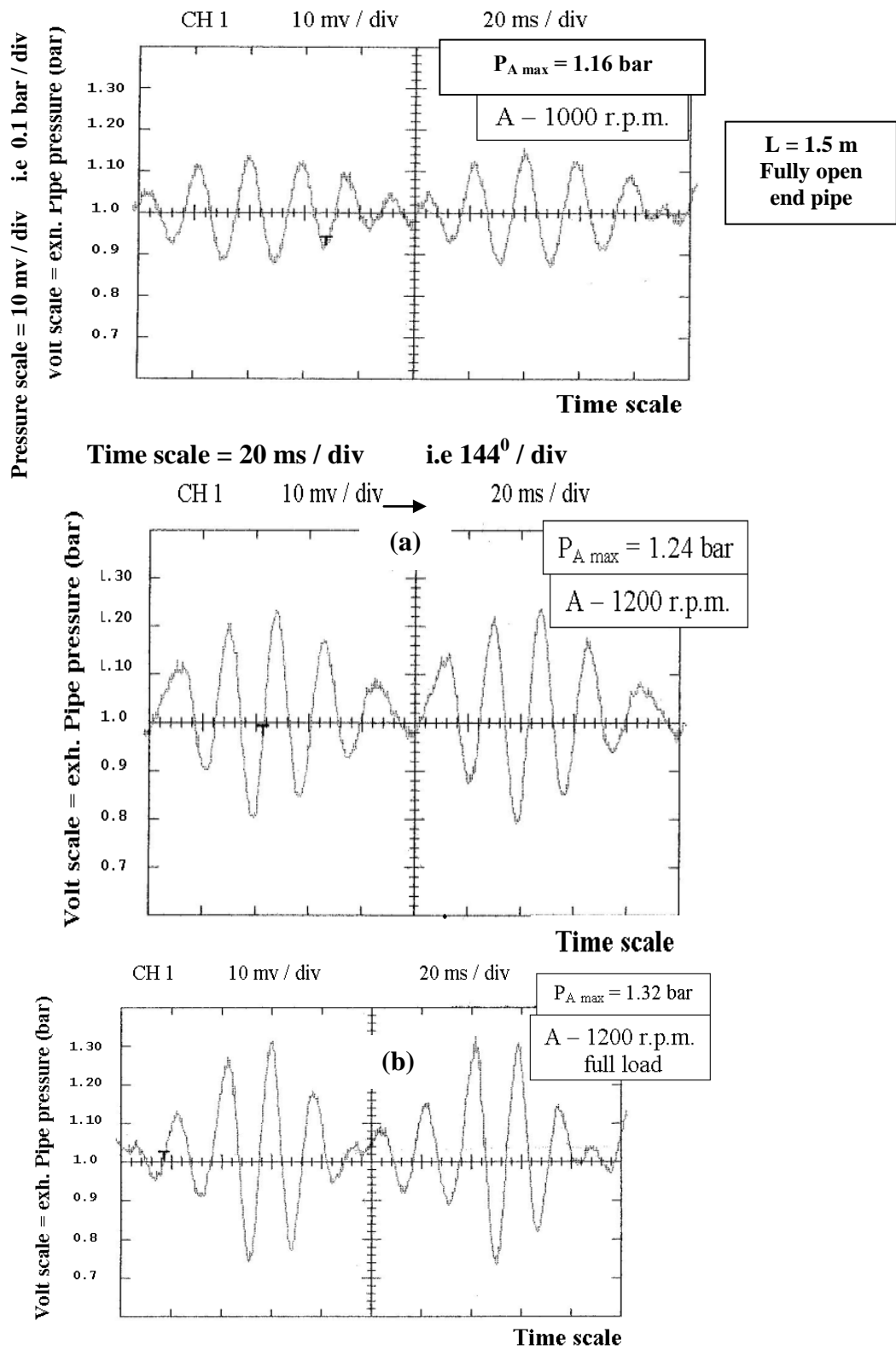


Fig. 15-a,b, c. Experimental results comparison of pressure wave variation at position "A" –with fully open end exhaust pipe $L = 1.5$ m.

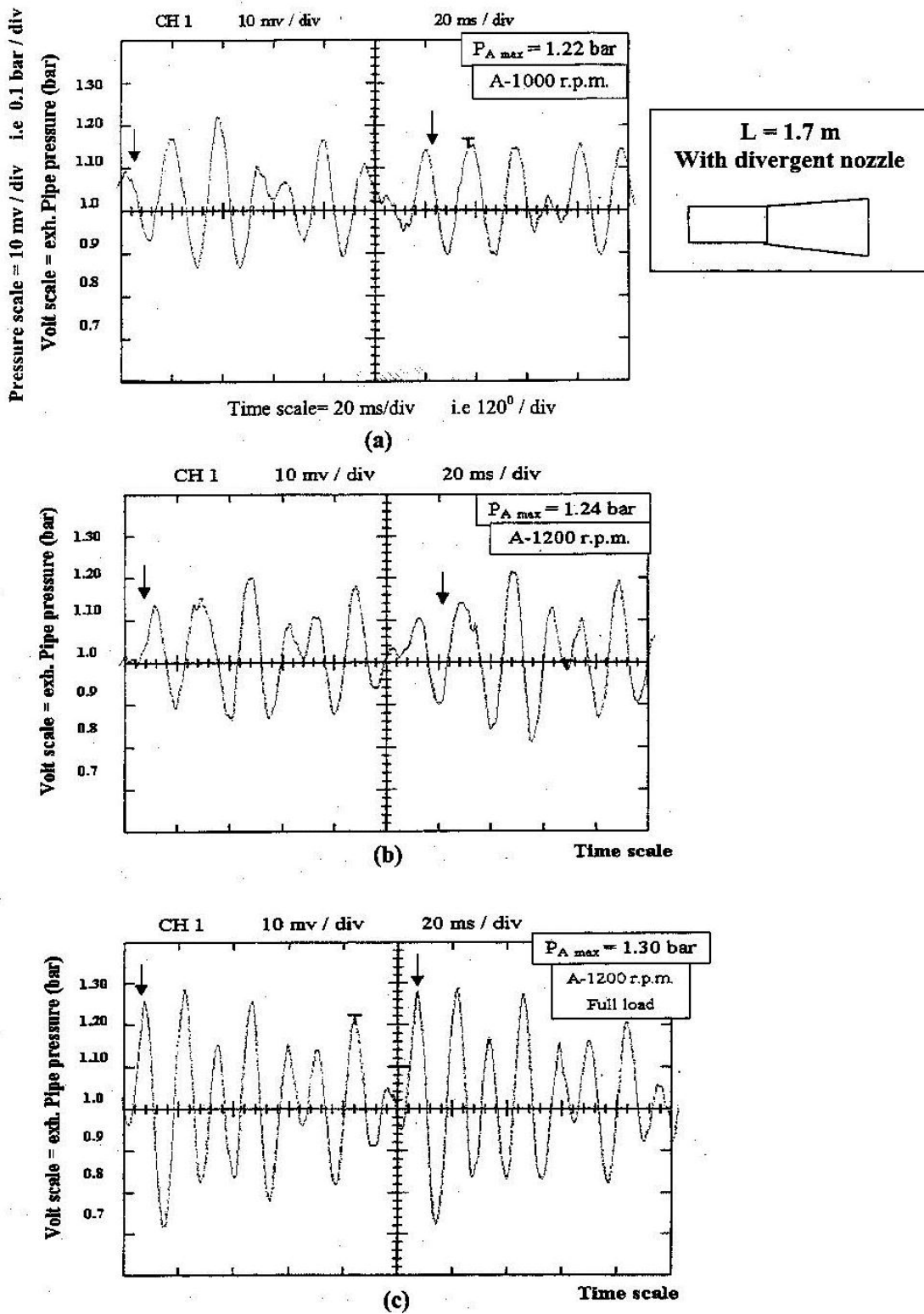


Fig. 16-a,b,c. Experimental results of pressure wave variation at position "A" –while engine firing at engine speed of 1000, 1200 r.p.m. and full (L = 1.7 m) with use of divergent nozzle

Table 3
Engine technical data and specifications

Type designation	1 NVD 12.5 SL
Operating principle	4-Stroke diesel
Number of cylinders	1, Vertical
Bore of cylinder	90 mm.
Stroke of piston	125 mm.
Swept volume	795 cm ³
Compression ratio	18 : 1
Combustion chamber	Eddy chamber
Cooling system	Air cooling with axial blower
Valves	1 inlet and 1 exhaust overhead valve each
Running – in out put (HP) / Engine speed	4.5 / 6.0 (HP) 1500 / 2000 r.p.m
Injection nozzle	Type SD 2 Z 45
Injection pressure	100 atm.
Valve cycle periods referred to crank shaft degrees	Inlet valve opens 15° 46' before T.D.C <ul style="list-style-type: none"> • Inlet valve closes 55° 46' after B.D.C. • Exhaust valve opens 55° 32' before B.D.C. • Exhaust valve closes 15° 32' after T.D.C
Fly wheel diameter = 460 m.m	

Table 4
Comparison of the predicted results of numerical solution and the measured data for peak pressure at position "A" and "B" engine firing test – exhaust pipe length $L = 1.0$ m

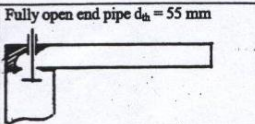
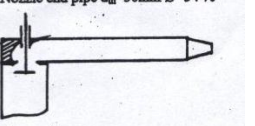
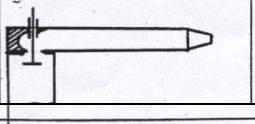
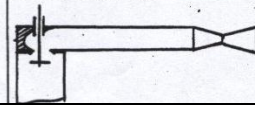
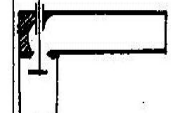
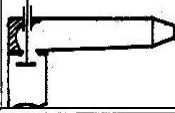

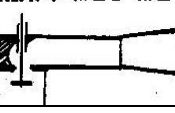
Test No.	Exhaust pipe condition	Const. Torque-speed 1000 r.p.m.				Const. Torque-speed 1200 r.p.m.			
		Experimental result		Numerical result		Experimental result		Numerical result	
		P_A max	P_B max	P_A max	P_B max	P_A max	P_B max	P_A max	P_B max
1	 Fully open end pipe $d_n = 55$ mm	1.16	1.10	1.15	1.10	1.15	1.14	1.20	1.12
2	 Nozzle end pipe $d_n = 30$ mm $\theta = 54$ %	1.10	1.08	1.15	1.10	1.12	1.12	1.2	1.125
3	 Nozzle end pipe $d_n = 20$ mm $\theta = 36$ %	1.14	1.12	1.15	1.10	1.12	1.12	1.2	1.125
4	 Conv.Div.end pipe $d_n = 20$ mm $\theta = 36$ %	1.12	1.13	1.15	1.10	1.14	1.14	1.2	1.125

Table 5
Comparison between experimental and numerical results for pressure wave variation at position "A"-pipe length 1.5 m – with different end conditions

Test no.	Exhaust pipe configuration	Engine firing speed 1000 r.p.m.		Engine firing speed 1200 r.p.m.		Engine full load. experimental results P_A max
		P_A max experimental	P_A max Numerical	P_A max Experimenta l	P_A max numerical	
5	Fully open end exhaust pipe $L=1.5$ m 	1.22	1.25	1.24	1.3	d1.32
6	Nozzle end exhaust pipe $d_n = 30$ mm $\theta = 54$ % 	1.18	1.25	1.15	1.3	1.26
7	Nozzle end exhaust pipe $d_n = 20$ mm $\theta = 36$ % 	1.16	1.25	1.2	1.3	1.28
8	Divergent nozzle end total cone 10° $t=0.7$ m $L=1.7$ m 	1.22	---	1.24	---	1.30

8. Conclusions and recommendations

In this study the unsteady flow through the exhaust system of internal combustion engines was stimulated by a simple one-dimensional homentropic model, the model employs data derived from the actual dimensions of the test diesel engine. The pressure wave was recorded experimentally through a single exhaust pipe during engine motoring and engine firing conditions with use of a different exhaust pipe end configurations. A comparison between the calculated results and measured data gives the following conclusions:-

1. The calculated maximum pressure levels were in most cases higher than the measured value due to neglecting the entropy gradient in the numerical solution.
2. The experimental results show that the pressure wave action through exhaust system

depends on pipe length, engine speed and load, pipe end configuration and valve area ratio.

3. The analysis of the experimental results show that the pressure wave action through exhaust system can affect the engine performance either adversely or positively depending on the above given factors, the optimum conditions can be approached by phasing the expansion wave reflection to match the exhaust stroke period, which can be attained either by control the exhaust valve timing or by control the exhaust pipe length as a function of engine speed.

4. The result analysis showed that by inserting a divergent section at exhaust pipe end, high amplitude of expansion wave reflection was created, which improve the pressure wave events through exhaust system.

Table 6
Comparison of engine performance while engine running at different engine loads and with different exhaust system configurations

Exhaust system configuration	Engine running condition						
	½ load – speed 1200 r.p.m.			Full load – speed 1200 rp.m.			
	Fuel kg/hr.	Thermal eff. ξ_{thb} %	Excess air factor “ λ ”	Fuel kg/hr.	Thermal eff. ξ_{thb} %	Excess air factor “ λ ”	
1 Engine original exhaust pipe with use exhaust silencer pipe length $L = 31$ cm	0.678	15.5	2	0.980	21.4	1.4	
2 Fully open end exhaust pipe without use exhaust silencer $L = 1.0$ m	0.582	18.0	3.4	0.790	26.6	2.5	
3 Fully open end exhaust pipe without exhaust silencer $L = 1.5$ m	0.510	20.6	3.6	0.850	24.7	2.1	
4 Nozzle end exhaust pipe $d_{th} = 30$ mm $\Phi = 54$ %	$L=1.0$ m	0.494	21.3	4.0	0.77	27.3	2.6
	$L=1.5$ m	0.480	21.9	3.8	0.85	24.7	2.1
5 Nozzle end exhaust pipe $d_{th} = 20$ mm $\Phi = 36$ %	$L=1.0$ m	0.490	21.4	4.0	0.78	26.9	2.6
	$L=1.5$ m	0.472	22.2	3.9	0.85	24.7	2.1
6 Convergent divergent nozzle end exhaust pipe $L = 1.0$ m $d_{th} = 20$ mm $\Phi = 36$ %	0.448	23.4	4.5	0.778	27.0	2.6	
7 Diffuser end exhaust pipe total cone angle $\theta = 10^\circ$ total pipe length with diffuser $L = 1.7$ m	0.480	21.9	3.8	0.850	24.7	2.1	

Nomenclature

A non dimensional speed of sound,
 A_A entropy level – non homentropic flow,
 F duct area "Benson",
 G friction force per unit mass,
 k is the ratio of the specific heats for a perfect gas,
 $J, N, M,$ End points of characteristics slopes on a fixed grid system,
 P pressure,
 q heat transfer per unit mass of the fluid flowing,
 R Gas Constant,
 s Entropy,
 t Time,
 u Gas velocity
 x Distance, and
 Z non-dimensional time.

Greek symbols

γ, k Specific heat ratio,
 ρ Gas density,
 $\Delta t, \Delta z$ time step size,
 α crank angle in degrees,
 ψ valve to pipe area ratio,
 λ_I Generalized characteristics (left to right), and
 λ_{II} Generalized characteristics (right to left).

Subscripts

evo Denotes exhaust valve open,
 evc Denotes exhaust valve closed,
 I Denotes Generalized Riemann, characteristic from left to right "+ve",
 II Denotes Generalized Riemann, and

characteristic from right to left "-ve",

Superscripts

", * Denotes non dimensional variables.

References

- [1] F.K. Bannister, "Influence of Pipe Friction and Heat Transfer on Pressure Waves in Gases, Effects in a Shock Tube", Journal of Mechanical Engineering science, Institution of Mechanical Engineers, Vol. 6 (3), pp. 278–292 (1964)
- [2] S. Earnshaw, on. "The Mathematical Theory of Sound". Pro. Roy. Soc. (1984).
- [3] B. Riemann, "Uber Die Fortpflanzung Ebener Luftwellen Von Endlicher Schwingungsweite", Bott. Abh. 8. (Math) (1885).
- [4] R. De Haller, "The Application of a Graphic Method to Some Dynamic Problems in Gases". Sulzer Technical Review 1, 6 (1945).
- [5] E. Jenny, "Uni-Dimensional Transient Flow with Consideration of Friction, Heat Transfer, and Change of Section", Brown Boveri Review, Vol. 37 (11), pp. 447 – 461 (1950).
- [6] W.A. Woods and S.R. Khan, "An Experimental Study of Flow through poppet valves", Proc. I. E., 180, 3N, 32 (1965 – 66).
- [7] Benson, R.S. Galloway, K. and Pick, R. "A Comparison of Measured and Calculated Indicator Diagrams During the Gas Exhaust Period in a Large Low_Speed Diesel Engine", B.S.R.A. Report No. ME. 529/IC (1982).
- [8] L.J. Kastiner, T.J. Williams and J. B. White, "Poppet Inlet Valve Characteristics and Their Influence on the Induction Process". Proc. Instn. Mech. Engr., Vol. 178, pt. 1 (36) – 64, pp. 955-74 (1963).
- [9] A.H. Shapiro, The Dynamics and Thermodynamics of Compressible fluid Flow, Vol. 1 and 2 Ronald Press Co (1954).
- [10] Roland Benson. "Thermodynamics and Gas Dynamics of Internal Combustion Engine". Vol. 1, Oxford (1982).
- [11] Marzouk, Awaad and A.F. Abdel Wahab, "A Comparative Study of Some Finite Difference Schemes in an Unsteady Discontinuous Compressible_Flow Field", Bulletin of Fac. of Alex. Univ., Vol. 33 (3) (1994).
- [12] D.B. Spalding and R. Issa "Unsteady Compressible Frictional Flow with Heat Transfer". J. Mech. Eng. Sci, Vol. 14. (6), (1974).
- [13] R.S. Benson, R.D. Garg and D. Wollatt, "A Numerical Solution Unsteady problems". Int. J. Mech. Sci., 6, pp. 117-144 (1964).
- [14] R.S. Benson, "Numerical Solution of one Dimensional Non-Steady Flow with Supersonic and Subsonic Flows and Heat Transfer", Int. J. Mech. Sci., Vol. 14, pp. 635-642 (1972).

Received June 8, 2004

Accepted August 12, 2004